AIP Journal of Applied Physics

Spectral characteristics of continuous wave broadband from a fiber laser with a low dispersion fiber in the cavity

Deepa Venkitesh and R. Vijaya

Citation: Journal of Applied Physics **104**, 053104 (2008); doi: 10.1063/1.2973458
View online: http://dx.doi.org/10.1063/1.2973458
View Table of Contents: http://scitation.aip.org/content/aip/journal/jap/104/5?ver=pdfcov
Published by the AIP Publishing

Spectral characteristics of continuous wave broadband from a fiber laser with a low dispersion fiber in the cavity

Deepa Venkitesh[1,2] and R. Vijaya[1,a)]
[1]*Department of Physics, Indian Institute of Technology-Bombay, Powai, Mumbai 400076, India*
[2]*Department of Physics, VES College of Arts, Science and Commerce, Sindhi Society, Chembur, Mumbai 400071, India*

(Received 12 March 2008; accepted 23 June 2008; published online 3 September 2008)

The spectral width of the continuous wave broadband generated in an erbium doped fiber ring laser containing a dispersion shifted fiber (DSF) in a filterless cavity is found to be governed by the nature of the gain spectrum of the doped fiber, in addition to the nonlinear effects. This dependence is studied experimentally with different lengths of the doped fiber and the DSF. Spectral broadening is demonstrated in the conventional (*C*) and long wavelength (*L*) bands using pump powers less than 200 mW, with an appropriate choice of cavity parameters. The generated broadband is demultiplexed in the *C*-band to prove its utility in optical communication systems. © *2008 American Institute of Physics*. [DOI: 10.1063/1.2973458]

I. INTRODUCTION

Different schemes for spectral broadening, multiline generation, and supercontinuum generation from an erbium doped fiber (EDF) ring laser (EDFRL) have been studied in the past in both the continuous wave (cw) and mode locked operations due to their relevance in diverse fields such as long haul fiber optic communication systems, spectroscopy, optical fiber sensors, component testing, and fiber optic gyroscopes. Both multiwavelength and broadband emissions have been achieved by cooling the EDF to 77 K (Refs. 1 and 2) using frequency shifting techniques[3,4] or by invoking different kinds of nonlinearities such as stimulated Brillouin scattering,[5] Raman Scattering,[6–8] and four wave mixing[9–11] (FWM) and by using specialty fibers.[12–15] Most of the cw supercontinuum generation schemes which utilize the nonlinear effects in fibers use very high pump powers of the order of watts.[15–17] Dispersion shifted fibers (DSFs) have been used as the nonlinear medium for demonstrating multiline generation through FWM of the wavelengths selected by the multiline filters or multiple Bragg gratings incorporated into the cavity.[10,11]

In this paper, we investigate the mechanism of spectral broadening in a cw-EDFRL, with the inclusion of DSF in the cavity in a *filterless configuration* for pump powers less than 200 mW. The absence of a frequency selective filter in this configuration enables the utilization of the large number of longitudinal modes that are naturally supported by the cavity toward nonlinear mixing processes. The multiple FWM processes occurring between these closely spaced longitudinal modes in the DSF result in spectral broadening throughout the gain spectrum of the EDF. The focus of this paper is to highlight the mechanism of spectral broadening by comparing the experimental results with the estimated *small-signal gain* spectrum of the doped fiber and to identify the appropriate cavity parameters for achieving large spectral widths with relatively low pump powers. Though the system is gain saturated in the steady state, the nature and the extent of broadening due to the increase in pump power are experimentally found to be guided by the nature of the small-signal gain due to the filterless configuration employed here.

II. EXPERIMENTAL SETUP

The experimental setup consists of a typical unidirectional ring cavity with a small length (*L*) of an EDF pumped by a laser operating at 980 nm.[18,19] A fraction (*R*) of the output power from the fiber is fed back to the input through a directional coupler to complete the ring cavity structure. *R* is chosen to be 0.99 to ensure maximum intracavity power for enhanced nonlinear processes. *L*, *R*, and the intracavity attenuation decide the wavelength of operation of a filterless laser.[19–23] The output is observed on an optical spectrum analyzer, which has a resolution bandwidth of 0.1 nm. Keeping *L* and *R* constant, a tunable laser is demonstrated by introducing additional loss (α) using a wavelength insensitive variable optical attenuator in the cavity.[24] It has been demonstrated previously that lasing is not restricted to the prominent peaks at 1530 and 1560 nm in the amplified spontaneous emission spectrum for a filterless laser. In a filterless ring cavity, all the wavelengths fed back at the input undergo multiple passes through the cavity and the lasing wavelength is the one for which the gain matches the cavity losses. Initially, the mode corresponding to the peaks in the gain spectrum would experience the maximum gain, but its gain drops fast due to saturation. This transient effect is practically not observable. The mode which has sufficient gain to counter the cavity losses is supported for lasing. The lasing wavelength of a filterless laser is decided by the length of the doped fiber, the reflectivity, the nature of the small-signal gain spectrum, and the cavity losses. Such a laser is tunable throughout the gain spectrum of the EDF, with the appropriate choice of cavity parameters.[24–26]

a)Author to whom correspondence should be addressed. Electronic mail: rvijaya@phy.iitb.ac.in.

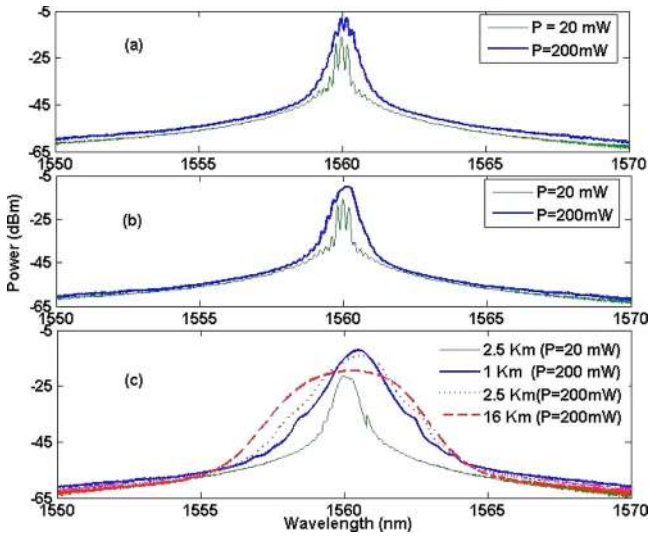

FIG. 1. (Color online) Spectral output of the EDFRL with (a) no additional fiber inserted in the cavity, (b) 2 km of SMF, and (c) different lengths of DSF inserted in the cavity. *P* indicates the pump power in each case.

III. RESULTS AND DISCUSSION

For a given cavity configuration, the linewidth of the filterless laser increases significantly with pump power, and the extent of this increase is decided by the wavelength of operation.[27] This natural linewidth of the laser is one of the primary factors that influence the extent of spectral broadening when a DSF is introduced into the fiber ring cavity. In order to quantify the extent of broadening due to the nonlinear effects, the spectral width is measured with different lengths of DSF introduced into the cavity.

Figure 1(a) shows the output spectrum of the EDFRL, with $L=4.7$ m, with no additional intracavity elements. It is observed that the linewidth, measured at 20 dB below the maximum power, is <1 nm at a pump power (P) of 20 mW (thin green line) and it increases to about 2 nm at $P=200$ mW (thick blue line). The increase in linewidth with an increase in pump power is attributed to the multiple FWM processes between the surviving longitudinal modes[28,29] rather than to the increased noise due to spontaneous emissions.[30] The frequency separation between the longitudinal modes being small, phase matching between these frequencies is significant enough to result in an efficient mixing process, leading to a measurable increase in linewidth, even in the absence of a significant length of nonlinear fiber in the cavity.

A standard single mode fiber (SMF) (with zero dispersion wavelength of 1312 nm) with length of 2 km is now introduced into the cavity. Figure 1(b) shows the output of the laser in this case. It is observed that the spectral width is similar to that in Fig. 1(a). A large dispersive phase introduced by the SMF hampers the phase matching in the FWM. On the other hand, introduction of a nonlinear medium into the cavity would result in the enhancement of these FWM processes. Figure 1(c) shows the output spectra when different lengths of DSF (zero dispersion wavelength at 1544 nm) are introduced into the cavity, with α adjusted in each case so that the center wavelength of lasing (λ_c) is the same in each case. Propagation through DSF results in improved phase matching efficiencies in an enhanced spectral width of the cw output, thus ratifying the concept of nonlinear mixing between the multiple longitudinal modes. Further increase in the length of DSF increases the interaction length for the nonlinear processes, resulting in enhanced FWM efficiency and in a spectrally broader output. The 20 dB spectral spread is 3 nm for a DSF length of 1 km, while it is 4 nm for a DSF length of 2.5 km and 6 nm for a DSF length of 16 km, as can be seen in Fig. 1(c). The power at λ_c is reduced for longer lengths due to the redistribution of powers within the supported longitudinal modes through FWM.

In order to analyze the effect of FWM on the spectral features throughout the emission range of the fiber, a fixed length of 1 km of DSF is chosen and α is varied, so as to tune the λ_c. The results are shown in Fig. 2. For all values of α, increase in pump power results in increased spectral width. However, the extent of this broadening is specific to a given wavelength range and a maximum spread of 28 nm is observed in the case of $\alpha=0.5$ dB with $\lambda_c=1585$ nm. This result indicates that, in addition to the nonlinear mixing ef-

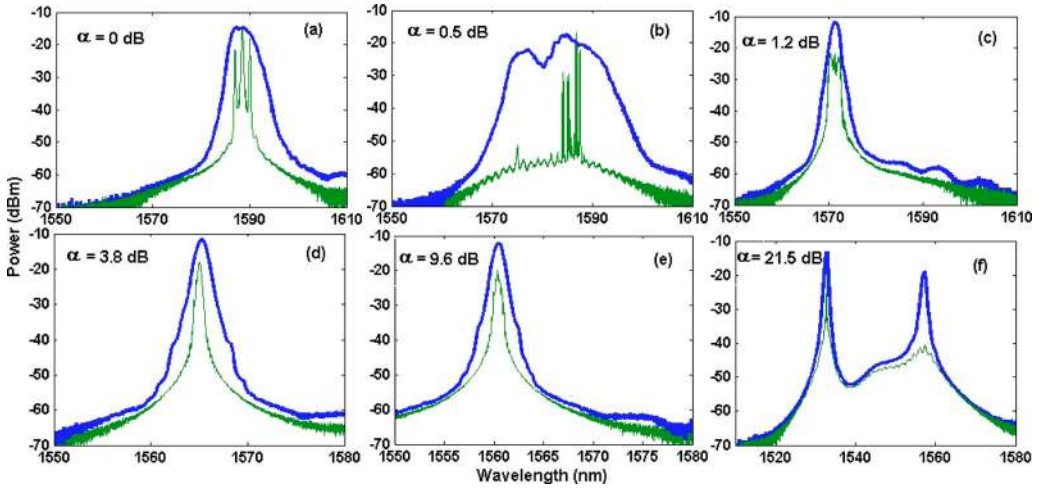

FIG. 2. (Color online) Spectral output from the EDFRL, with EDF of length of 4.7 m and DSF of length of 1 km. Thin green and thick blue lines correspond to low (20 mW) and high (200 mW) pump powers, respectively.

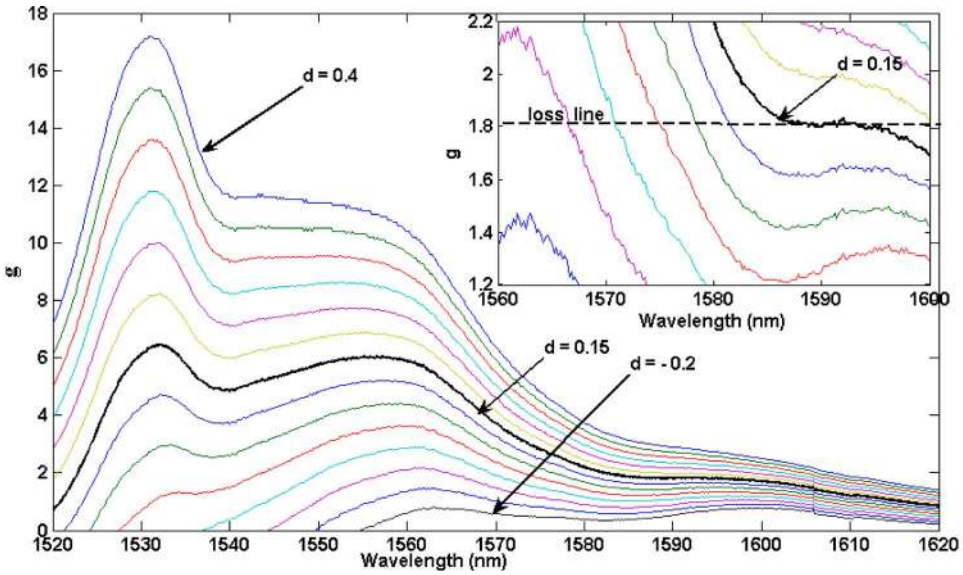

FIG. 3. (Color online) Gain coefficient calculated for inversions from −0.2 to 0.4 in steps of 0.05. Inset shows the gain coefficient for a smaller wavelength range.

fects, the spectral features of broadening are significantly influenced by the emission and absorption characteristics of the fiber.

These features can be investigated through the spectral dependence of the small-signal gain coefficient (g) on the wavelength independent average inversion levels (d) in the fiber calculated using

$$g = \Gamma_s \rho L \left[\sigma_e(\lambda_s)\left(\frac{1+d}{2}\right) - \sigma_a(\lambda_s)\left(\frac{1-d}{2}\right)\right], \tag{1}$$

where Γ_s accounts for the transverse overlap of the signal beam with the dopant ions, while σ_e and σ_a are the emission and absorption cross sections of the EDF at the signal wavelength λ_s, and ρ is the dopant concentration of the fiber used.[31] It should be emphasized that, in the absence of an intracavity filter or a seed wavelength in the cavity, the lasing process is initiated from the amplified spontaneous emission, whose characteristics are very well represented by the small-signal gain calculated using Eq. (1). Hence, even though the propagating field in the cavity experiences saturated gain in steady state, the above analysis based on the small-signal gain is still valid for the interpretation of spectral characteristics of the laser in the filterless configuration.

Figure 3 shows a family of curves indicating the spectral dependence of g for the EDF with length of 4.7 m calculated for different values of d. For a given d, the lasing wavelength is the one for which the g matches the net intracavity loss (shown as the loss line in the inset of Fig. 3). d can be increased by increasing the pump power in an experiment. Since the nature of the spectral dependence of g changes significantly with d, it is useful to obtain an approximate estimate for d for a given experimental condition in order to identify the wavelength of interest in the family of curves shown in Fig. 3. For $\alpha = 21.5$ dB, simultaneous lasing is observed at ~1530 and 1560 nm in the experiments [as can be seen in Fig. 2(f)]. The gain spectrum corresponding to $d = 0.15$ (shown as a bold line in Fig. 3) can compensate for this loss and an additional loss of about 7 dB in the cavity (attributed to the wavelength division multiplexer, isolator, and other splices) and simultaneously allow lasing at the two specified wavelengths. The same inversion level of $d = 0.15$ can result in lasing at 1590 nm at a smaller value of α. For example, in the case of $\alpha = 0$ dB, the lasing wavelength is close to 1590 nm [seen in Fig. 2(a)], corresponding to an additional loss of 7 dB in the cavity. The gain spectrum at an inversion of $d = 0.15$ shown in the expanded scale in the inset of Fig. 3 indicates the lasing wavelength as 1590 nm. d is numerically small due to the large absorption in the C-band. It should be reiterated that the estimate of d is not exact since the contribution due to nonlinear mixing and its effect on inversion and the spectral response of the other intracavity components are not included in this model. However, this estimate is useful to interpret the spectral width obtained at the output.

The natural linewidth of the laser is decided by the flatness of the gain coefficient, which is different in different wavelength ranges, as can be seen in Fig. 3. As α increases, the lasing wavelength decreases, corresponding to an upward shift in the loss line. This results in the deviation from the flatter regions of the gain spectrum, and hence, in smaller values of spectral spread, especially for the values of d corresponding to our experiment and as can be seen in Figs. 2(c)–2(e). For $d = 0.15$, the g in the region of 1570–1600 nm is flat, resulting in a larger number of participating modes in multiple FWM processes and an enhanced spectral spread, as can be seen in Fig. 2(b). Thus, the key to obtain the largest spectral spread at relatively lower values of pump power is to operate at those inversion levels and intracavity loss values where the gain spectrum is flat and to simultaneously provide a sufficient length of the nonlinear fiber. Broadband generation is thus favored in the L-band under this scheme.

In order to validate the above inference on the influence of the small-signal gain in the spectral broadening process, similar aspects are studied for a longer EDF length of $L = 12$ m. The results displayed in Fig. 4 show certain unique features of broadening. The spectrum seen at the higher pump power is not symmetrical about the lasing wavelength obtained at a lower power. The broadening is more toward

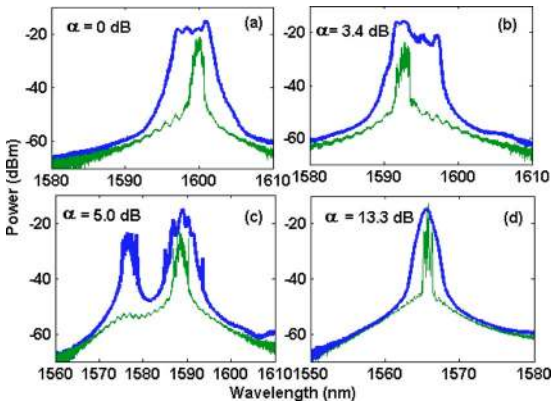

FIG. 4. (Color online) Spectral output from the EDFRL, with EDF of length of 12 m and DSF of length of 1 km. Thin green and thick blue lines correspond to low (20 mW) and high (250 mW) pump powers, respectively.

the shorter wavelengths (anti-Stokes region) in Figs. 4(a) and 4(c), while it is toward the longer wavelengths (Stokes region) in Fig. 4(b). The spectrum is uniformly broadened in the case of Fig. 4(d). This feature can also be explained using the nature of the gain spectrum of the EDF. Figure 5 shows a family of curves representing g calculated for $L=12$ m and at different values of d. For the experimental conditions corresponding to this length, one can identify that the inversion corresponds to d values between −0.1 and 0. With the longer length of the doped fiber, there is a significant absorption in the C-band in the initial section of the fiber, resulting in a quasi-four-level operation of the laser. This explains the smaller values of average inversion for this configuration. In the case of Fig. 4(a), the value of λ_c is 1600 nm at the lower pump power. Since the gain curves are flatter on the lower wavelength side of 1600 nm in Fig. 5, the spectral broadening is skewed toward the anti-Stokes wavelength region for these values of d. On the contrary, in the case of Fig. 4(b), $\lambda_c=1592$ nm at lower powers, and hence, with the increase in pump power, the broadening is toward its longer wavelength region due to the flatness of g in that region for $d=0$. For wavelengths between 1560 and 1580 nm, g monotonously decreases for positive d. Hence, the contribution to spectral broadening is primarily due to nonlinear effects, resulting in a uniform increase in the spectral spread about the

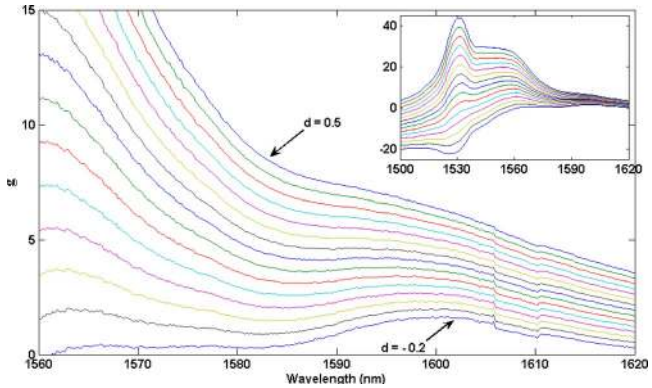

FIG. 5. (Color online) Gain coefficient calculated for EDF $L=12$ m for inversions from −0.2 to 0.5 in steps of 0.05. Inset shows the gain coefficient for a larger wavelength range.

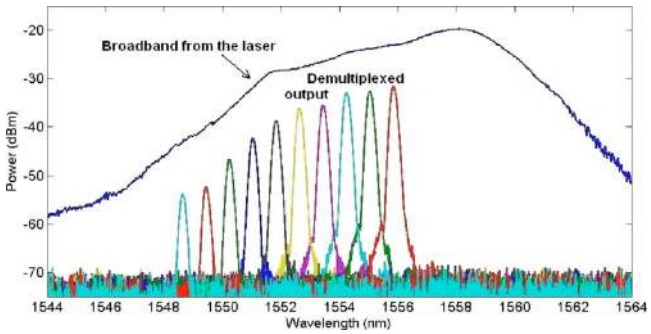

FIG. 6. (Color online) Broadband generated from the EDFRL and the demultiplexed output with an interchannel spacing of 100 GHz.

λ_c, as can be seen in Figs. 2(c)–2(e) and 4(d). g is also found to have dips/inflections for $d>-0.2$ between 1575 and 1590 nm, and between 1530 and 1550 nm (seen in Fig. 3 and in the inset of Fig. 5), resulting in significant dips in the broadband seen in Figs. 4(c) and 2(f), respectively. The extent of broadening can be significantly increased with the use of larger pump powers and highly nonlinear fibers. The extent of broadening is different in the different wavelength ranges, implying that the coherence characteristics of the output are also expected to be different in different wavelength ranges.

A potential application for such a spectral broadband output from a cw laser is in fiber optic communication, where individual wavelengths can be extracted from the generated spread spectrum by using a suitable demultiplexer at the output of the cavity. Since the longitudinal mode spacing of this laser oscillator is in the megahertz range, the demultiplexed channels at an interchannel separation of, say, 100 GHz may be incoherent to a certain extent. In addition, the contribution from multiple nonlinear mixing processes can result in significant amplitude fluctuations. In order to assess the utility of the demonstrated broadband source for spectral splicing in the conventional communication band, the broadband is generated in the C-band. An EDF of smaller dopant concentration, with a length of 5 m, is used as the gain medium and a DSF with a length of 0.5 km is used as the nonlinear medium in this experiment. The generated broadband is spectrally sliced using a commercially available demultiplexer in the wavelength range of 1548.52–1555.75 nm with an interchannel spacing of 100 GHz on the International Telecommunications Union (ITU) grid in the C-band. The broadband from the laser and the demultiplexed output are shown in Fig. 6.

It is observed from the ten demultiplexed channels that the maximum power in each channel follows the spectral profile of the generating broadband and there are no significant fluctuations in the power of each channel. Contrary to the schemes which rely only on multiple nonlinear processes by propagation of a high power signal through a low dispersion fiber, the amplitude fluctuations are expected to be minimal in the present scheme since the nonlinear processes are aided by the intrinsic gain inside the ring cavity at the generated wavelengths. Each of the demultiplexed channels can be further subjected to modulation with a pseudorandom bit generator and subsequently tested for parameters such as eye opening penalty and bit error rate for its applicability in data

transmission systems. Possibility of generation of the spread spectrum in different wavelength bands without the use of specialty fibers or high powers make this design versatile.

IV. CONCLUSION

The mechanism of spectral broadening in EDF lasers due to the inclusion of a DSF in the cavity is studied for pump powers less than 200 mW. The salient feature of this work is the use of a variable optical attenuator in conjunction with a DSF to obtain broadband emission at relatively low pump powers throughout the emission spectrum of EDF. In cw operation, in addition to the contribution from the multiple FWM between the surviving longitudinal modes, the nature and extent of spectral broadening are strictly guided by the small-signal gain of the laser. This aspect is explained using the spectral dependence of the gain coefficient of the doped fiber at different levels of inversion.

ACKNOWLEDGMENTS

The authors gratefully acknowledge the partial financial support from the University Grants Commission and the Council of Scientific and Industrial Research, Government of India.

[1]J. Chow, G. Town, B. Eggleton, M. Isben, K. Sugden, and I. Bennion, IEEE Photonics Technol. Lett. **8**, 60 (1996).
[2]S. Yamashita and K. Hotate, Electron. Lett. **32**, 1298 (1996).
[3]J. N. Maran, S. LaRochelle, and P. Bernard, Opt. Lett. **28**, 2082 (2003).
[4]R. Slavik and S. LaRochelle, Opt. Lett. **27**, 28 (2002).
[5]M. P. Fok and C. Shu, Opt. Express **14**, 2618 (2006).
[6]M. González-Herraez, S. Martin-Lopez, P. Corredera, M. L. Hernanz, and P. R. Horche, Opt. Commun. **226**, 323 (2003).
[7]W. Zhang, Y. Wang, J. Peng, and X. Liu, Opt. Commun. **231**, 371 (2004).
[8]A. A. Babin, D. V. Churkin, A. E. Ismagulov, S. I. Kablukov, and E. V. Podivilov, Opt. Lett. **31**, 3007 (2006).
[9]X. Liu, X. Zhou, and C. Lu, Opt. Lett. **30**, 2257 (2005).
[10]Y. G. Han and S. B. Lee, Opt. Express **13**, 10134 (2005).
[11]Y. G. Han, T. V. A. Tran, and S. B. Lee, Opt. Lett. **31**, 697 (2006).
[12]X. Liu, X. Xhou, X. Tang, J. Ng, J. Hao, T. Y. Chai, E. Leong, and C. Lu, IEEE Photonics Technol. Lett. **17**, 1626 (2005).
[13]A. Zhang, M. S. Demokan, and H. Y. Tam, Opt. Commun. **260**, 670 (2006).
[14]S. Pan, C. Lou, and Y. Gao, Opt. Express **14**, 1113 (2006).
[15]J. H. Lee, Y. Takushima, and K. Kikuchi, Opt. Lett. **30**, 2599 (2005).
[16]J. H. Lee and K. Kikuchi, Opt. Express **13**, 4848 (2005).
[17]J. H. Lee, K. Katoh, and K. Kikuchi, Opt. Commun. **266**, 681 (2006).
[18]A. Bellemare, Prog. Quantum Electron. **27**, 211 (2003).
[19]D. Venkitesh and R. Vijaya, Proc. SPIE **6796**, 679611 (2007).
[20]A. Bellemare, M. Karasek, C. Riviere, F. Babin, G. He, V. Roy, and G. W. Schinn, IEEE J. Sel. Top. Quantum Electron. **7**, 22 (2001).
[21]T. Rosadiuk and J. Conradi, IEEE Photonics Technol. Lett. **5**, 758 (1993).
[22]P. Franco, M. Midrio, A. Tozzato, M. Romagnoli, and F. Fontana, J. Opt. Soc. Am. B **11**, 1090 (1994).
[23]X. Dong, P. Shum, N. Q. Ngo, H.-Y. Tam, and X. Dong, J. Lightwave Technol. **23**, 1334 (2005).
[24]V. Deepa and R. Vijaya, Appl. Phys. B: Lasers Opt. **89**, 329 (2007).
[25]G. R. Lin, J. Y. Chang, Y. U. Liao, and H. H. Lu, Opt. Express **14**, 9473 (2006).
[26]G. R. Lin, H. H. Lu, and J. Y. Chang, IEEE Photonics Technol. Lett. **18**, 2233 (2006).
[27]V. Deepa and R. Vijaya, J. Appl. Phys. **102**, 083107 (2007).
[28]V. Roy, M. Piche, F. Babin, and G. W. Schinn, Opt. Express **13**, 6791 (2005).
[29]J.-C. Bouteiller, IEEE Photonics Technol. Lett. **15**, 1698 (2003).
[30]A. Yariv, *Quantum Electronics*, 2nd ed. (Wiley, New York, 1975).
[31]E. Desurvire, *Erbium Doped Fiber Amplifiers: Principles and Applications* (Wiley, New York, 1994).